

## Synthesis and characterization of elemental silver clusters on silver (I, II, III) oxide clathrate films, $\text{Ag}^0/\text{Ag}_7\text{O}_8\text{H}(\text{CO}_3)$ , by the chemical bath deposition technique

E. Fernández-Díaz<sup>a,b</sup>, T. Mendivil-Reynoso<sup>c,\*</sup>, L. P. Ramírez-Rodríguez<sup>c</sup>,  
R. Ramírez-Bon<sup>d</sup>, S. J. Castillo<sup>a</sup>, R. Ochoa-Landín<sup>c</sup>

<sup>D</sup>epartment of Physics Research, Sonora University, p.o. Box 5-088, ZIP code  
83000, Hermosillo, Sonora, México

<sup>b</sup>Physics Laboratory of Hermosillo Institute of Technology, Av. Tecnológico, ZIP  
code 83170, Hermosillo, Son., México

<sup>c</sup>epartment of Physics, Sonora University, p.o. Box 1626, ZIP code 83000  
Hermosillo, Sonora, México

<sup>d</sup>IPN Investigation Centre and Advanced Studies, Campus Queretaro, p.o. Box. 1-  
798, ZIP code 76001, Querétaro, Qro., México

Chemical bath deposition technique at room temperature proved to be efficient in synthesizing elemental silver clusters on Silver (I, II, III) oxide clathrate films,  $\text{Ag}^0/\text{Ag}_7\text{O}_8\text{HCO}_3$ . The set of samples was prepared for 30, 60, 90 and 120 minutes. All films exhibited a yellowish-brown color and presented good adherence to the corning glass substrate. The direct band gaps values were 3.77 to 3.82 eV. A cubic crystallographic structure was determined with the usage of TEM; while SEM was used for the observation of their morphology which showed a very homogenous flat background with a distribution of metallic silver clusters with irregular shape was growing.

(Received July 13, 2021; Accepted November 23, 2021)

**Keywords:** Chemical bath deposition, Silver oxide clathrate, TEM, SEM

### 1. Introduction

The optical and electrical properties of silver have been studied because of its multiple applications and also, because humanity has always wanted to understand and describe the phenomena that occurs in nature. Furthermore, due to the appearance of d-shell in silver material there are several ways in which it can be found in nature [1], for instance:  $\text{AgO}$ ,  $\text{Ag}_2\text{O}$ ,  $\text{Ag}_3\text{O}$  and  $\text{Ag}_2\text{O}_3$ . In particular, because the applications have been treated as  $\text{AgO}$  and  $\text{Ag}_2\text{O}$ , or as cathodic materials in Zn-silver oxide batteries [2-6], silver alloys as optical data storage [7], or in medicine [8], Ag nanoparticles result interesting like antimicrobial agents [9]. A form of silver that is also worth mentioning is clathrate-type silver oxide, which has superconductor properties [10]. Some authors have synthesized silver (I, II, III) oxide clathrate  $\text{Ag}_7\text{O}_8\text{HCO}_3$  by ozonolysis and by anodic oxidation of silver (I) in a suspension of  $\text{Ag}_2\text{CO}_3$  in aqueous  $\text{AgF}$  solution [11]. In turn, the silver clathrate  $\text{Ag}_7\text{O}_8\text{NO}_3$  and  $\text{Ag}_7\text{O}_8\text{HSO}_4$  have been synthesized by the photoelectrochemical technique [12]. In this paper, we report the characterization of  $\text{Ag}^0/\text{Ag}_7\text{O}_8\text{HCO}_3$  films and powders synthesized by using the chemical bath deposition technique. The films were deposited on glass substrates at room temperature, and using a new recipe of syntheses.

### 2. Experimental

The  $\text{Ag}^0/\text{Ag}_7\text{O}_8\text{HCO}_3$  films were deposited on corning glass substrates from aqueous solutions. The reactive solution was prepared in a 100 ml beaker by sequential addition of 5 ml of 0.1 M  $\text{AgNO}_3$ , 5 ml of 0.3 M  $\text{KOH}$ , 2 ml of 1 M Triethanolamine, 80 ml of deionized water and 6 ml of a Rongalite solution. Four substrates were placed in the reaction beaker and removed from

---

\* Corresponding author: temis\_83@hotmail.com

the solution after 30, 60, 90 and 120 minutes. The  $\text{Ag}^0/\text{Ag}_7\text{O}_8\text{HCO}_3$  films had a yellowish brown color and were homogeneous, with a good adherence to the substrate.

The optical absorption spectra of the films were obtained by diffuse reflectance spectroscopy (DRS) measurements (Varian Cary 5-e spectrometer) using the Kubelka–Munk theory spectrophotometer. SEM images were taken in a JEOL JSM 5400LV electron microscope. The crystalline structure of the films was determined by X-ray diffraction (XRD) and the patterns were measured in an X-ray diffractometer Bruker D8 ADVANCE. Raman was carried on in a XploRA RAMAN microscope HORIBA system and the FTIR spectrum was recorded using a PerkinElmer UATR Spectrum Two. A Field Emission Electron Probe Micro Analyzer (*FE-EPMA*) was also used for identified the composition of the sample.

### 3. Results

The first characterization presented here will be the X-Rays Diffraction. As can be observed, Figure 1 (a) shows a powder pattern at the top and layers at the bottom. All layers patterns show four peaks, the most intense are around 38.12 degree, these four peaks correspond to diffraction lines (111), (200), (220) and (311) associated to the crystal cubic structure of silver, corresponding with the crystallographic chart PDF # 65-2871. The increment of the peak intensities related with the reaction times can also be seen. Using the Debye-Scherrer method (111), an average crystal size of 62 nm was obtained. The optical absorption spectra of the set of films are shown in figure 1 (b), depicting absorption among 22% to 50% when the wavelengths are in the 318 to 800 nm range. The band gap was estimated using the Tauc method for direct band gap, in the inset the spectra Absorption (A) vs wavelength ( $\lambda$ ) were converted to  $(\alpha h\nu)^2$  vs energy (hv), where  $\alpha$ , h, and  $\nu$ , are the absorbance, the Planck's constant and the frequency, respectively. The absorption edge is placed among 300 to 318 nm and the calculated values were 3.82, 3.79, 3.77 and 3.82 eV for the 30, 60, 90 and 120 minutes samples, respectively.

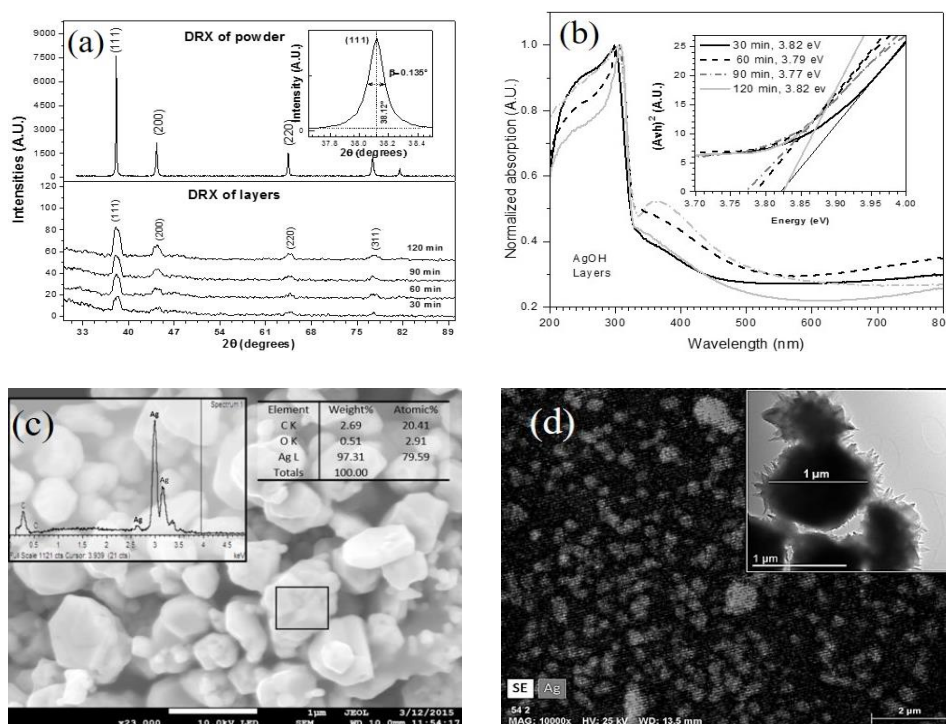


Fig. 1 (a) XRD spectra, (b) optical absorption spectra, (c) SEM and EDS and (d) FE-EPMA of the obtained material.

On the other hand, in figure 1 (c) the SEM image of the residual powder is shown, after having been cleaned. Here it can be observed that such powders are formed from grains or clusters of different sizes and shapes. The insets of figure 1 (c), display the EDS analysis (left) and the composition percentage (right), where the highest percentage for silver can be observed. In figure 1 (d) the morphology images are shown. They are formed by two characterizations, containing as a main micrograph a microprobe image, the film presents a homogenous background and no pores, i. e., it does not have pin holes (black color), over the background a distribution of unconnected clusters grow with irregular shapes and different sizes, which was identified as silver by *FE-EPMA*. The inset figure corresponds to an image of TEM that depicts a few individual silver clusters surrounded by nanocrystals, which were unidentified in the DRX patterns, although their crystalline structure could be identified using HTRM.

In Figure 2 (a) we find the HRTEM of nanocrystals observed on the inset figure 1(d). Here the left side is a contrast image where we can appreciate crystallographic planes in different directions. The labeled planes, 1-11; 311; 220; 13-1, in the up-right quadrant were found by applying Fourier Transform in the selected quadrant, which is shown in the figure 2 (b). From these plane,s a set of interplanar distances and angles were calculated, which are in very good agreement with PDF # 53-1292, corresponding to cubic silver hydrogen oxide carbonate,  $\text{Ag}_7\text{O}_8\text{H}(\text{CO}_3)$ . In other words, the material hereby synthesized id Ag; however, it is surrounded by silver calthrate which in this case is not detected by the XRD, this is due because there are more crystalline planes associates with Ag than with calthrate silver. Nonetheless, this is observed by TEM, since the measurements are local.

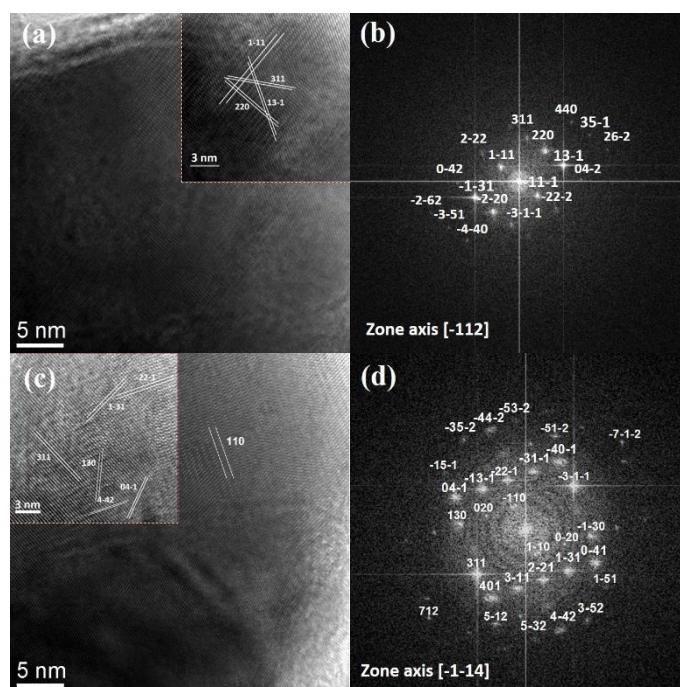


Fig. 2. HRTEM micrograph image (left side) and FFT image of the HRTEM (right side), first test region, Zone axis  $[-112]$  and  $[-1-14]$ .

The FTIR spectra, figure 3 (a), were compared with various related research [14-15] and have shown certain concordance. In our analysis we divide the complete range in two regions I and II, the first one corresponding to functional groups from 4000 to 1500  $\text{cm}^{-1}$ , and the second from 1500 to 500  $\text{cm}^{-1}$  for the synthesized compound involved, which is often called the finger print region of the compound (being, in our case, silver composite layers or silver nanoparticles deposited as LDH). Table 1 shows some functional groups identified on the synthesized composite: silver clathrate with silver clusters.

Table 1. Shows some conformed functional groups on the synthesized compound.

Wavenumbers (cm <sup>-1</sup> )	3344	2921, 2851, 1363, 1178, 883, 756	1747	1587	1036	618
Functional Group	O-H	C-H	C=O	C-C	C-N	-C≡C-H: C-H

Figure 3 (b), shows the two series of the four Raman spectra, accommodated by pairs, which correspond to the two different wavelengths of excitation (lasers in 647 and 435 nm). As can be observed, the Raman peaks intensities were more intense when the red laser was used. The Raman spectra of our samples could correspond to silver clathrate compound, due to the silver clusters immersed in it.

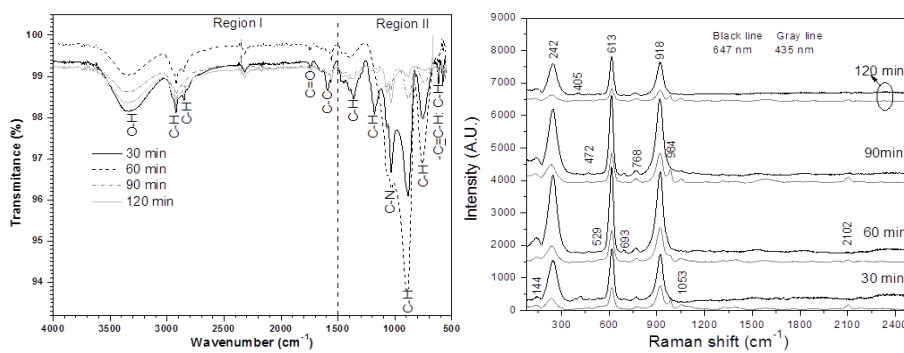


Fig. 3. (a) set of FTIR spectra to identify the presence of some functional groups, (b) Raman Spectra of the sample by a using a laser 647 nm and 435 nm.

#### 4. Conclusions

Silver composite was obtained, where silver has to be bonded in three different oxidation states. The process used is different than those reported both in articles and in patents, and has proven to be simple, short and inexpensive. The coating obtained is beige, well adhered to the substrate, and presents high electrical resistance. SEM images proved the continuity and homogeneity of the silver clathrate layers. The direct band gap values were calculated and located between 3.77 to 3.82 eV. The vibrational, TEM and EDS techniques help prove that our material is not certainly pure silver, as was revealed by XRD. This research proposes some Raman peaks signals for the obtained composite  $\text{Ag}^0/\text{Ag}_7\text{O}_8\text{HCO}_3$ , where the  $\text{Ag}^0$  induces an enhancement of the silver clathrate.

#### Acknowledgments

CONACyT by the financial support of the student Enrique Fernandez Diaz and financial postdoctoral position to PhD. Temistocles Mendivil Reynoso PhD. Enrique Quiroga González, from Instituto de Física de la Benemérita Universidad Autónoma de Puebla (SEM and EDS); PhD. Vicente Garibay Febles from Laboratorio de Materiales Nanoestructurados y Microscopia del Instituto Mexicano del Petróleo (TEM).

## References

- [1] N. R. C. Raju, K. J. Kumar, A. Subrahmanyam, *Journal of Physics D: Applied Physics* **42**, 135411 (2009).
- [2] Y. Wan, X. Wang, S. Liu, Y. Li, H. Sun, Q. Wang, *Int. J. Electrochem. Sc.*, **8**, 12837 (2013).
- [3] A. P. Karpinski, S. J. Russell, J. R. Serenyi, J. P. Murphy, *J. Power Source* **91**(1), 77 (2000).
- [4] D. F. Smith, J. A. Gucinski, *J. Power Sources* **80**, 66 (1999).
- [5] D. F. Smith, C. Brown, *J. Power Sources* **96**, 121 (2001).
- [6] G. I. Waterhouse, J. B. Metson, G. A. Bowmaker, *Polyhedron* **26**(13), 3310 (2007).
- [7] H. U. S. Ichtenberger, *Patent Application* **10**(930), 178 (2005).
- [8] M. S. Antelman, *US Patent* 5.211.855 (1993).
- [9] Y. Delgado-Beleño, C. E. Martínez-Núñez, N. S. Flores-López, A. Meza-Villezcás, L. P. Ramírez-Rodríguez, R. Britto Hurtado, M. Flores-Acosta, M. Cortez-Valadez, *Journal of Electronic Materials* **50** (10), 1 (2021).
- [10] K. Kawashima, M. Ishii, S. Date, T. Tsutsumi, H. Okabe, J. Akimitsu, *Physica C: Superconductivity* **460**, 542 (2007).
- [11] M. Jansen, S. Vensky, *S. Zeitschrift für Naturforschung B* **55**(9), 882 (2000).
- [12] R. Tanaka, R. Takahashi, S. Takata, M. Lippmaa, Y. Matsumoto, *CrystEngComm*. **17**(19), 3701 (2015).
- [13] F. Soofivand, M. Salavati-Niasari, F. Mohandes. *Journal of Industrial and Engineering Chemistry* **20**(5), 3780 (2014).
- [14] T. C. Prathna, N. Chandrasekaran, A. M. Raichur, A. Mukherjee, *Colloids and Surfaces B: Biointerfaces* **82**(1), 152 (2011).
- [15] M. M. Rahman, S. B. Khan, A. Jamal, M. Faisal, A. M. Asiri, **192**, 122 (2012).
- [16] F. Zare, M. Ghaedi, A. Daneshfar, S. Agarwal, I. Tyagi, T. A. Saleh, V. K. Gupta, *Chemical Engineering Journal* **273**, 296 (2015).
- [17] D. A. Islam, D. Borah, H. Acharya, *RSC Advances* **5**(17), 13239 (2015).
- [18] F. Chen, R. E. Wasylshen, *Magnetic Resonance in Chemistry* **48** (4), 270 (2010).